

Conceptual Aircraft Hinge Moment Measurement System

A Senior Project

presented to

the Faculty of the Aerospace Engineering Department  
California Polytechnic State University, San Luis Obispo

In Partial Fulfillment

of the Requirements for the Degree

Bachelor of Science in Aerospace Engineering

by

Erin M. Hambrick and Nicole M. Thomason

June 2010

© 2010 Hambrick and Thomason

# Hinge Moment Measurement System for Wind Tunnel Aircraft Models

Erin M. Hambrick<sup>1</sup> and Nicole M. Thomason<sup>1</sup>  
*California Polytechnic State University, San Luis Obispo, CA, 93407*

The Conceptual Aircraft Hinge Moment Measurement System (CAHMMS) was designed, prototyped, and validated to improve hinge moment estimates early in the design process. Validation was performed by integrating CAHMMS with a test wing and conducting wind tunnel tests to compare the expected theoretical, historical, and Computational Fluid Dynamics (CFD) predictions to the experimental results. As CAHMMS is an external measurement system, interference effects at the connection points were investigated. Further studies were undertaken to verify the CFD predictions with the experimental hinge moment measurements. Hinge moment results from the experimental data and the theoretical data closely correlated with less than 5% difference, validating the CAHMMS design. Over simplification of boundary layer modeling and mesh generating techniques are attributed to the poor correlation of the analytical data. Understanding of the CAHMMS system and its interactions with the test surface can be further determined through finer mesh generation and more precise boundary layer modeling using the CFD analytical technique.

## Nomenclature

$C_d$	= drag coefficient
$C_h$	= hinge moment coefficient
$C_l$	= lift coefficient
$H$	= hinge moment (lbf-in)
$S$	= area (in <sup>2</sup> )
$c$	= chord (in)
$d_A$	= distance from the free end of the lever arm to the free end of the control surface (in)
$d_l$	= distance from hinge point to control rod attachment point (in)
$d_M$	= distance from hinge point of the control surface to hinge point of transducer lever arm (in)
$q$	= dynamic pressure (psf)
$\alpha$	= angle of attack (deg)
$\Phi_{CR}$	= angle of the transducer lever arm (deg)
$\Phi_{CS}$	= angle of the control surface (deg)
$\delta$	= angle of deflection (deg)

## I. Introduction

THIS report details the validation testing of the Conceptual Aircraft Hinge Moment Measurement System (CAHMMS). The purpose of the system is to provide accurate low speed wind tunnel measurements of control surface hinge moments on small scale aircraft models. A summary of the project background, motivation, design process, and experimental testing will also be explained while focusing on the analytical Computational Fluid Dynamics (CFD) solutions.

### A. Motivation

This project was sponsored by Lockheed Martin Aeronautics Company in Palmdale, CA as a submission by the California Polytechnic State University San Luis Obispo (CPSLO) Society of Women Engineers (SWE) to the

---

<sup>1</sup> Student, Aerospace Engineering Department, 1 Grand Ave., Student Member.

national SWE Team Tech Competition. The CPSLO SWE design team worked closely with Lockheed Martin Aeronautics to design and test CAHMMS. CAHMMS was presented at the 2009 SWE Conference and won the first place award in the Team Tech Competition. Further examinations of the wind tunnel test results as well as studies in DATCOM and CFD were undertaken by the authors for the purpose of this report.

The hinge moment is the moment acting about the hinge line of a control surface that must be overcome to move the control surface when a pilot exerts force command on the control stick. The force exerted by the pilot is augmented with mechanical ratios provided by the control surface actuators. Actuators are implemented and sized based on the magnitude of the force required to rotate the control surface about the hinge. At any given dynamic pressure and Mach number, the hinge moment varies with angle of attack, control surface deflection, and trim tab deflection. The effects that contribute to the hinge moment are difficult to analytically predict but are necessary to properly design the aircraft control system.

Currently, hinge moments are not measured on conceptual aircraft models, as they cannot be discerned from the total forces measured by the sting balance during a wind tunnel experiment. Panel code analysis, some CFD, and existing wind tunnel and aircraft test data are used during the conceptual design process to conservatively approximate hinge moments. These estimation techniques often lead to overestimation of required control surface actuator size, increasing the weight and cost of the aircraft. Accurate hinge moment measurements on larger scale wind tunnel models do not typically occur until late in the design process if at all, potentially requiring costly design modifications and causing delay before the aircraft is put into production. The desire to improve hinge moment estimates early in the design process motivated the research to create CAHMMS. CAHMMS will allow for more accurate control surface actuator sizing during conceptual design, resulting in a more efficient and cost effective design process. Additionally, CAHMMS will facilitate trade studies to determine the effects of the control surface geometry on the magnitude of the hinge moment, allowing for actuator sizing during the conceptual design process.

The design requirements specified by Lockheed Martin Aeronautics and achieved by CAHMMS include measurement accuracy within 5% and a control surface deflection of  $\pm 30^\circ$ . CAHMMS also incorporates the desired ability of control surface actuation to change the deflection of the control surface remotely during wind tunnel testing.

Small scale conceptual aircraft models are grown using rapid prototype stereolithography (SLA) material. The typical control surfaces made of SLA material were assumed to have a 5 inch span, 2 inch chord, and 0.3 inch thickness. The aircraft models are tested in the 3 foot by 2 foot test section of the Lockheed Martin Aeronautics Low Turbulence Wind Tunnel (LTWT), Fig. 1, which allows model wing spans of up to 27 inches to be tested at angles of attack from  $-10^\circ$  to  $+22^\circ$  combined with angles of sideslip of over  $20^\circ$ .

## B. Apparatus

Due to the small scale of the aircraft models and the wind tunnel testing facility, CAHMMS was designed as an external measurement system. A torque transducer is used instead of the traditional strain gauges on an internal beam flexure. It is housed inside “the pod”, an egg shaped casing, and suspended above or below the aircraft model by a fully adjustable tripod connected to the model at three points spaced away from the control surface being measured. A connecting rod attaches the transducer to the control surface. A stepper motor is also located in the pod to allow for changes in the control surface deflection angle through movement of the control rod during testing. Figure 2 shows the internal components of “the pod.” The



**Figure 1. Lockheed Martin Low Turbulence Wind Tunnel**

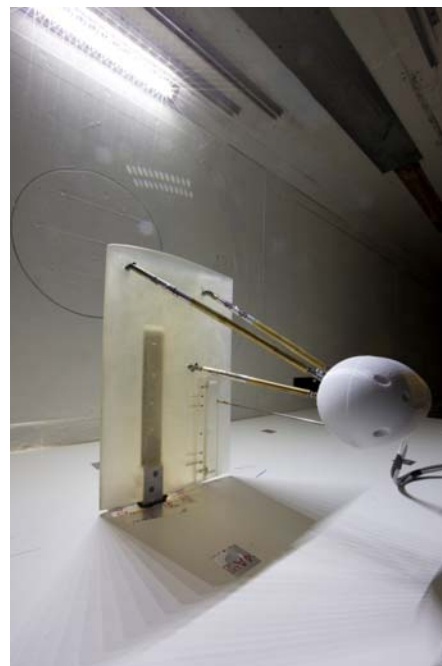


**Figure 3. CAHMMS attached to the test wing in the Lockheed Martin LTWT.**

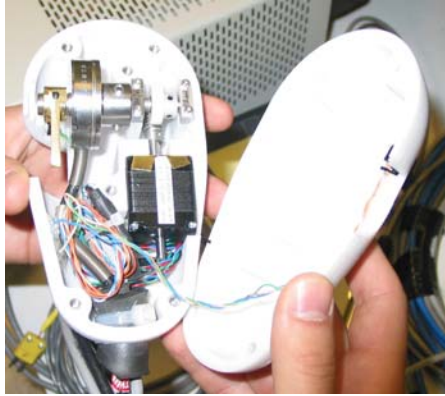


**Figure 2. Force transducer, lever arm, and stepper motor inside the pod of the CAHMMS measurement device.**

shape and placement of the pod were chosen based on basic aerodynamic principles and preliminary two dimensional CFD solutions.

The test wing, shown in Fig. 3 with CAHMMS attached in the LTWT, was constructed of SLA material. It was designed to both match the experimental wing used in TN 2080<sup>1</sup> at the reduced scale of typical Lockheed Martin Aeronautics aircraft models. The test wing section was a NACA 64A010 airfoil and contained a quarter-chord half-span inboard control surface.

## II. Analysis

The validation and verification of CAHMMS was done using CFD and the Lockheed Martin LTWT data compared against theoretical and historical predictions.

### A. Theoretical Prediction

The USAF Stability and Control Datcom, through the more user friendly Digital DATCOM<sup>3</sup>, provides predictions for hinge moment derivatives for a sealed control surface; however, these methods are limited to the range of control surface deflections and angles of attack for which the flow stays attached over the control surface. The sensitivity of trailing-edge controls to boundary layer separation and Reynolds number effects leads to non-linear hinge moments at moderate to large angles. Within small to moderate angles, the linear relationship of the hinge moment as a function of control surface deflection and angle of attack may be described as follows

$$C_h = C_{h_\alpha} \alpha + C_{h_\delta} \delta \quad (1)$$

The following equation calculates the non-dimensional hinge moment, where H is the hinge moment, q is dynamic pressure,  $S_f$  is flap area, and  $c_f$  is flap chord aft of the hinge line.<sup>1</sup>

$$C_h = \frac{H}{qS_f c_f} \quad (2)$$

### B. Historical Measurement

The explanations, experimental setup, and test conditions of NACA TN 2080 became the basis for the test wing and test conditions for CAHMMS.

Lift, drag, pitching moment, and flap hinge moment were measured for a wing with a plain flap in TN 2080. The investigation for TN 2080 was carried out in the NACA Langley 300mph, 7 by 10 foot wind tunnel using an unswept, untapered NACA 64A010 section wing with an aspect ratio of 3.13. Tests were performed at an average dynamic pressure of 100 psf, which corresponds to 0.27 M and a Reynolds number of 4.5 million as based on the wing mean aerodynamic chord of 2.5 feet. Tests included seven flap deflections between 0° and 60° performed through an angle of attack range from -4° to stall. The wind tunnel measurements indicate a turbulence factor close to unity.<sup>1</sup> The explanation of the interface geometry between the wall and the flap edge was unclear as to whether a gap existed. To obtain an undisturbed hinge moment measurement, there likely was some gap present. The hinge moments were measured with an internal strain gauge system mounted at the hinge line of the control surface.

### C. Analytical Prediction

Computational Fluid Dynamics (CFD) was used to analytically determine the flow conditions surrounding the CAHMMS device. A 2-dimensional and 3-dimensional model of the test wing and

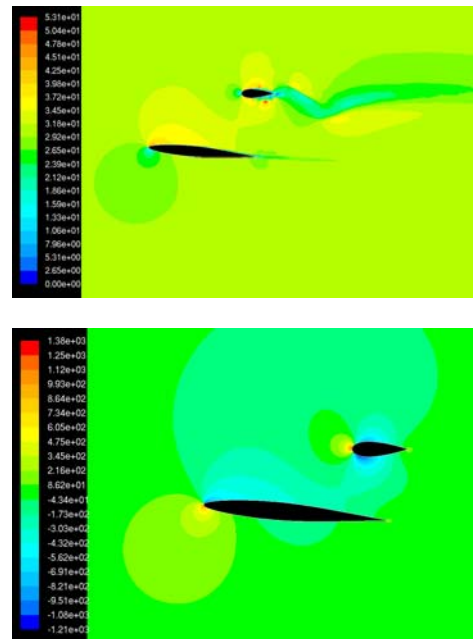


**Figure 4. Velocity (in/s) and pressure (psi) contours around a representative 2-D wing and pod for a viscid CFD case.**

CAHMMS were created using SolidWorks to define the geometry necessary to import into the flow solvers. The point coordinates for the NACA 64A010 representing the test wing and NACA 0028 representing the pod were used to make spline curves to shape the airfoils. The test wing curve was then extruded to represent the span of the wing while the CAHMMS curve was rotated to represent the thickness of the pod. The 3-dimensional model does not account for the flow circulation of an actual wing nor the holes and gaps necessary for connection points in the test wing.

Early in the CAHMMS design process, 2-dimensional CFD solutions were run to investigate the interference effects of the test wing and the pod of CAHMMS. Gambit was used as the meshing software for the 2-D cases to create boundary layers around the test wing and pod, and a triangular mesh grid that was then analyzed in the CFD software, Fluent. Meshing software breaks the air space surrounding objects of interest into small control volumes, creating a mesh. In complicated flow regions, a smaller mesh allows for more accurate predictions of flow characteristics. A CFD program can then calculate the flow properties of the mass flow through each of the control volumes. Adding up the characteristics for each control volume gives you an overall picture of what is happening to the flow surrounding the object of interest. Due to the limitations of a 2-dimensional solution, the tunnel walls and the connecting rod and tripod were not modeled. The separation distance between the two airfoils was investigated to determine the minimum height of the pod over the test wing without greatly affecting the flow over the wing, shown in Fig. 4.

Once preliminary 2-dimensional CFD computations were completed, further cases were conducted to determine the interaction of the pod with the wind tunnel wall boundary layer. ICEM software was used to create a 3-dimensional unstructured tetrahedral mesh around the test wing and CAHMMS. The dimensions of the LTWT test section were replicated to surround the test wing with CAHMMS. Again, solutions were obtained from Fluent. The test conditions of TN 2080 were used to analyze the flow. Figure 5 shows the inviscid solutions for the test wing with CAHMMS.

Next, further CFD cases were studied to obtain a viscous solution. This consisted of merging an unstructured tetrahedral mesh with a prism mesh built up along all surfaces to model the boundary layer, or the flow interaction with the surfaces. Figure 6 shows the viscous solution of the test wing alone run at the test conditions of the TN 2080. Figure 7 shows the viscous solution of the test wing with CAHMMS run at the test conditions of the LTWT.

When conducting their research regarding hinge moment prediction and measurement, Grismer concluded that “modeling wind tunnel walls produces significant effects in numerical solutions, and may be necessary when comparing with wind tunnel data.”<sup>2</sup> Therefore, it was desired to only solve the flow condition constrained by the wind tunnel geometry. The ease of an inviscid solution was also discounted as “inviscid solutions cannot provide accurate moments due to important viscous effects near the trailing edge of the control surface.”<sup>2</sup>

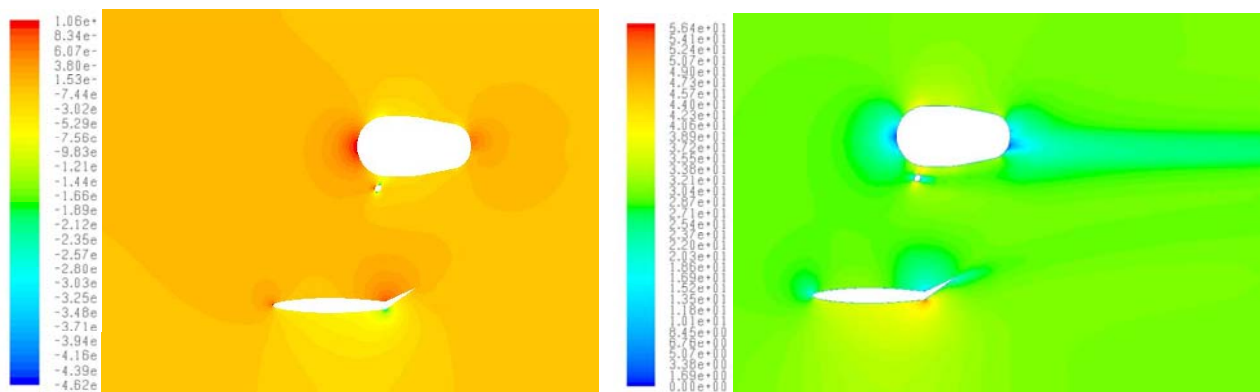


Figure 5. Pressure (psi) and velocity (in/s) contours of the wing with a flap deflection of 30°, the pod suspended above, and the rod attached in a 3-D inviscid CFD case.



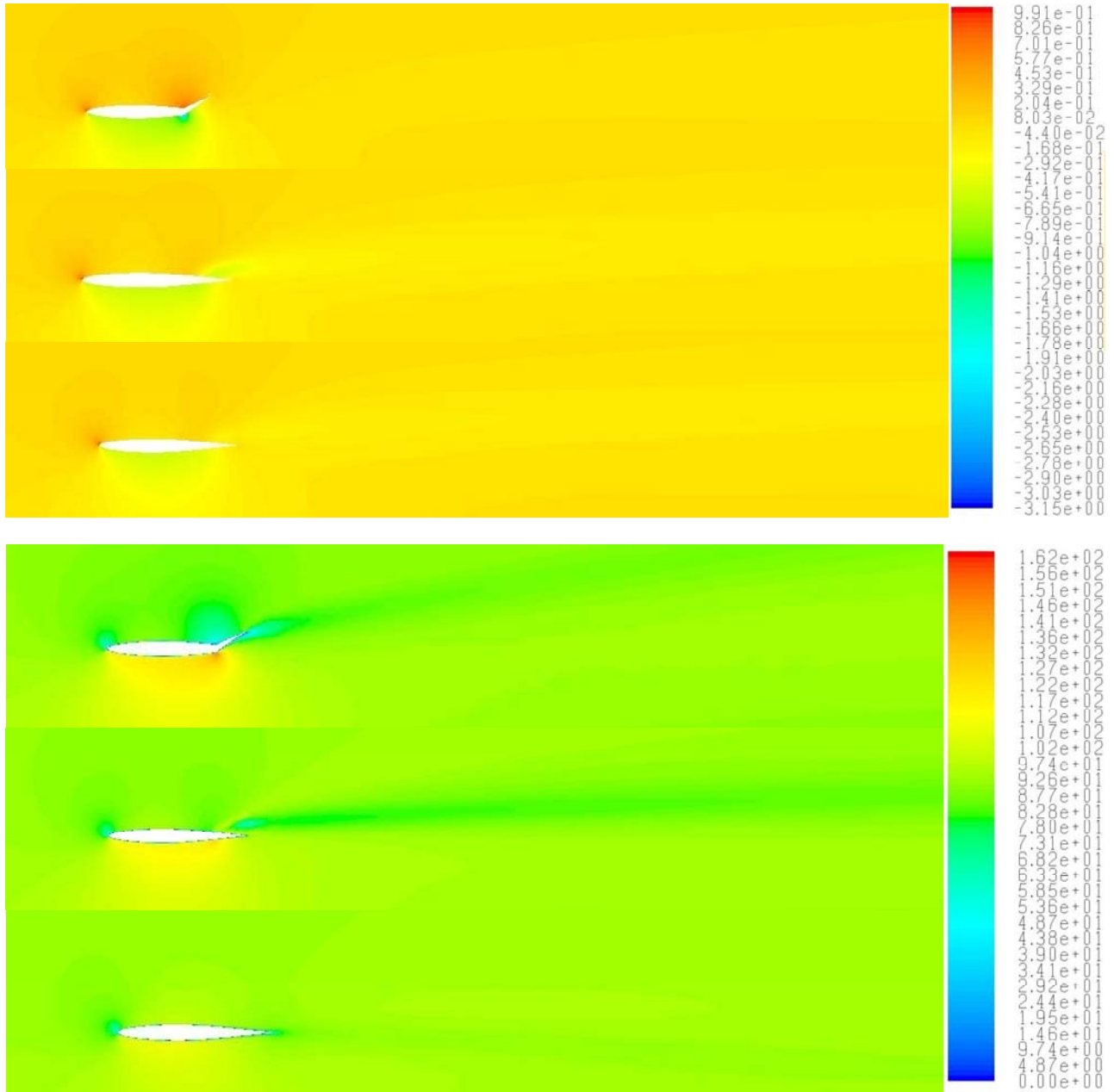


Figure 6. Pressure (psi) and velocity (in/s) contours of the wing with 30° flap deflection in a viscous CFD case.

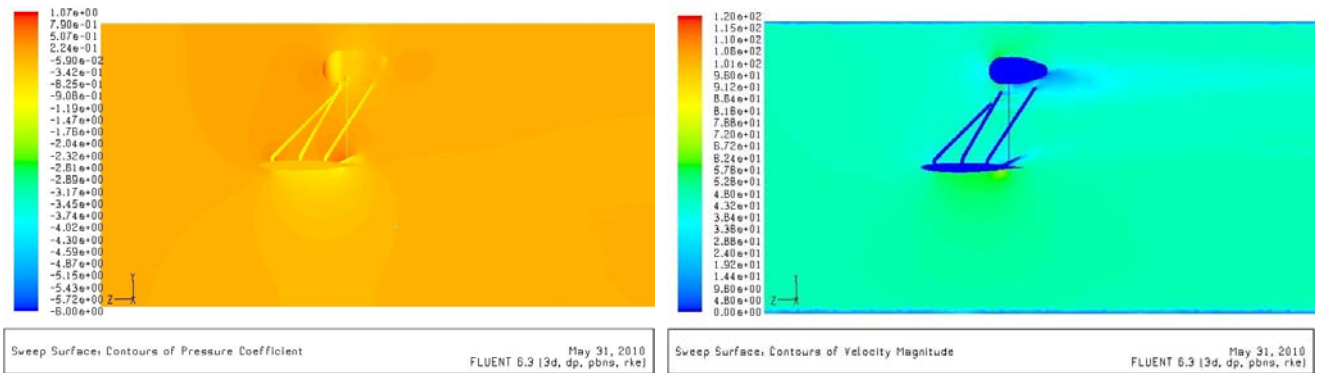


Figure 7. Pressure (psi) and velocity (in/s) contours of the wing with a flap deflection of 30° and CAHMMS attached.

#### D. Experimental Measurement

The test wing is a quarter scale model of the TN 2080 wing with the inboard half span flap. It measures 7.5 inches by 11.62 inches. The choice of the inboard flap gave the ability to mount the tripod legs of CAHMMS on the underside of the wing near the tip, reducing interference with the control surface. Mounting CAHMMS on the outboard portion of the wing increases the induced moment at the test wing to wind tunnel attachment point, but because of the small wing span in this case it is not a significant moment to interfere with data collection. However, the tripod attachment system allows for variability in attachment for future test setups.

TN 2080 states there is very large freestream turbulence in the wind tunnel, but does not specify any conditions of boundary layer transition. Assuming a turbulent boundary layer in the TN 2080 experiment, boundary layer trip dots were placed at 10% chord of the test wing model to induce turbulence. The test velocity was reduced to 56% due to the operating limitations of the LTWT at 30 psf. This takes the Reynolds number from 4.5 million down to 630,000 on the chord. The LTWT has a 0.1 inch gap between the flap edge and the tunnel wall.

Adjustments were made to the wind tunnel data to account for physical movement of the apparatus when wind forces were applied. A correction factor for vertical pod motion was calculated using Equation (3).  $\phi_{CR}$  is the angle of the transducer lever arm,  $\phi_{CS}$  is the angle of the control surface,  $d_l$  is the length of the transducer lever arm from the hinge point to the control rod attachment point,  $d_A$  is the distance from the free end of the control surface to the free end of the transducer lever arm, and  $d_M$  is the distance from the hinge point end of the control surface to the hinge point end of the transducer lever arm.

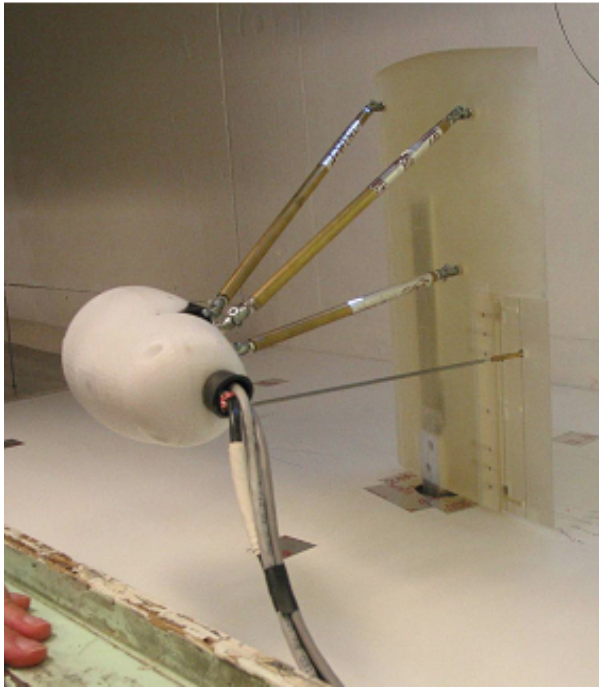
$$\phi_{CR} = \arctan\left(\frac{d_l \sin \phi_{CS} + (d_A - d_M)}{d_l \cos \phi_{CS}}\right) \quad (3)$$

A correction factor for change in pod angle due to force on the pod was determined using equation (4), where  $k_{TR}$  is the stiffness of the transducer lever arm.

$$\Delta \phi_{CR} = \Delta \phi_{CS} = \frac{M}{k_{TR}} \quad (4)$$

### III. Results

Figure 7 plots the LTWT experimental hinge moment measurement data and the TN 2080 hinge moment data at 8° angle of attack and a control surface deflection range from -30° to +30°. This shows the close correlation of the experimental wind tunnel data and the NACA TN 2080 data. The chart shows a difference of less than 5% for control surface deflections up to +10°, meeting the requirements set forth by Lockheed Martin. The data from +10° to +30° shows a consistent divergence from the TN 2080 data, underestimating the hinge moment by 12%.



**Hinge Moment Coefficient vs. Control Surface Deflection**

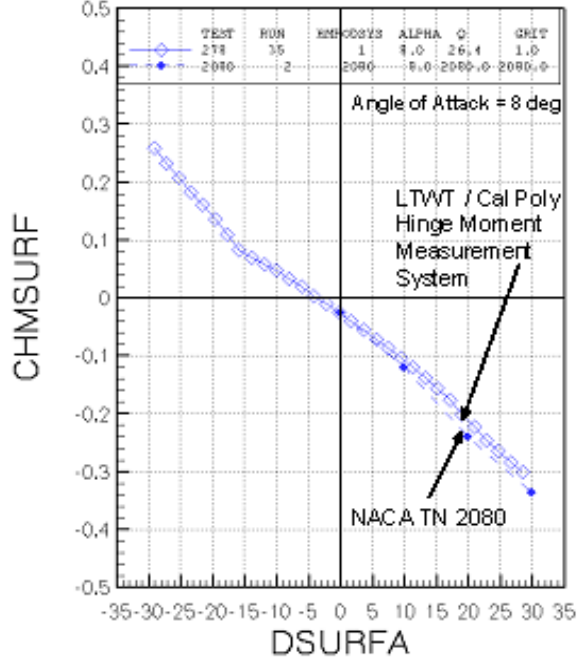


**Figure 7. Correlation of TN 2080 hinge moment data and experimental results from wind tunnel testing at the Lockheed Martin Low Turbulence Wind Tunnel.**

The wing lift and drag and the control surface hinge moment non-dimensional results for 0° angle of attack and 30° control surface deflection from each method are summarized in Table 1. The experimental hinge moment data from the wind tunnel test most closely correlates with the validation hinge moment data from the NACA TN 2080. The case of comparison represents the most extreme control surface deflection within the CAHMMS range of motion; nevertheless, the LTWT hinge moment measurement correlates with TN 2080 data within 7%. The LTWT test had to account for the effect of the pod by applying correction factors in determining the hinge moment solutions to compare with the TN 2080 tests which used an internal hinge moment measurement system. Because correction factors were not applied to the drag solutions, the experimental drag is much higher than historical data. The experimental increase in drag measured in the LTWT indicates that there is an effect of the pod on the wing. If the gap present in the LTWT was reduced, the hinge moment magnitude would increase toward the TN 2080 data.

**Table 1. Comparison of coefficients with analytical and experimental results.**

	$C_l$	$C_d$	$C_h$
<b>TN 2080</b>	0.38	0.06	-0.33
<b>DATCOM</b>	0.420	0.082	-0.426
<b>CFD wing only</b>	0.576	0.069	-0.441
<b>CFD with CAHMMS</b>	0.102	0.063	-0.260
<b>LTWT with CAHMMS</b>	0.322	0.163	-0.306

The overestimation of the hinge moment by the analytical methods, CFD and DATCOM, could be due to the complications in modeling the separation over the wing with a high flap deflection of 30°. With a fine tuned mesh and more precise boundary layer modeling, the analytical results obtained from CFD could be made more accurate and would be found to more closely correlate with the experimental and TN 2080 data. The correction factors developed and applied during the LTWT testing were not applied to the CFD results. In addition, the CFD test conditions represented the lower Reynolds number of the LTWT test rather than the higher Reynolds number of the TN 2080. CFD proved most valuable by adding the insight of flow visualization to examine the interference between the pod and tripod on the control surface of the wing and the high drag seen in the wind tunnel test case.



#### IV. Conclusion

CAHMMS provides accurate predictions of hinge moments for small scale aircraft models. Although CAHMMS is an external system and so does not have an effect on the aerodynamic characteristics of the test model, correction factors for the pod motion may be applied to the hinge moment measured to obtain accurate estimates within 5% for small deflections and within 12% for large deflections. This provides a significant cost benefit as control surface actuators may be accurately sized early in the design process. Furthermore, designers can utilize CAHMMS to conduct control surface trade studies on small scale aircraft models at a reduced cost and increased accuracy.

#### Acknowledgments

The authors would like to thank the CPSLO SWE Team Tech design team who took CAHMMS from concept to prototype, specifically Directors Nadia Shraibati and Alan Tepe; the CPSLO Aerospace Engineering Department who offered advice and lab access; and most of all the advisors at Lockheed Martin Aeronautics, specifically Mark Buchholz, who generously offered their expertise, equipment, and encouragement throughout the project.

#### References

- <sup>1</sup> Johnson, H.S., and Hagerman, J.R., "Wind-Tunnel Investigation at Low Speed of an Unswept Untapered Semispan Wing of Aspect Ratio 3.13 Equipped with Various 25-Percent-Chord Plain Flaps," NACA Technical Note 2080, Langley Aeronautical Laboratory, Langley Air Force Base, VA, Apr. 1950.
- <sup>2</sup> Grismer, M., Kinsey, D., Grismer, D., „Hinge Moment Predictions Using CFD“, AIAA 2000-4325, Air Vehicles Directorate, Air Force Research Laboratory, Wright-Patterson Air Force Base, OH, Aug. 2000.
- <sup>3</sup> Digital DATCOM, Software Package, Ver. 2.6, Holy Cows, Inc., Orlando, FL, 2010.
- <sup>4</sup> FLUENT, Software Package, Ver. 11.26-1, ANSYS, Inc., Canonsburg, PA, 2005.
- <sup>5</sup> Grismer, D., Grismer, M., Simon, J., Tinapple, J., „An Experimental Investigation of Factors Influencing Hinge Moments,” AIAA 2000-4016, Air Vehicles Directorate, Air Force Research Laboratory, Wright-Patterson Air Force Base, OH, Aug. 2000.
- <sup>6</sup> GAMBIT, Software Package, Ver. 2.4.6, ANSYS, Inc., Canonsburg, PA, 1988-2010.
- <sup>7</sup> Hoak, D.E., et al, "USAF Stability and Control Datcom," AFWAL-TR-83-3048, October 1960 (revised April 1978).
- <sup>8</sup> ICEM, Software Package, Ver. 11.0.1, ANSYS, Inc., Canonsburg, PA, 2007.
- <sup>9</sup> SolidWorks, Software Package, SP. 5.0, Dassault Systèmes SolidWorks Corp., Concord, MA, 1995-2008.